

Dual element (C-Cl) isotope approach to distinguish abiotic reactions of chlorinated methanes by Fe(0) and by Fe(II) on iron minerals at neutral and alkaline pH

Diana Rodríguez-Fernández[†], Benjamin Heckel[§], Clara Torrentó[‡], Armin Meyer[§], Martin Elsner[§], Daniel Hunkeler[‡],
Albert Soler[†], Mònica Rosell[†], Cristina Domènech[†]

[†]Grup MAiMA, Mineralogia Aplicada, Geoquímica i Geomicrobiologia, Departament de Mineralogia, Petrologia i
Geologia Aplicada, Facultat de Ciències de la Terra, Martí Franquès s/n, Universitat de Barcelona (UB), 08028
Barcelona, Spain.

[§]Institute of Groundwater Ecology, Helmholtz Zentrum München, 85764 Neuherberg, Germany.

[‡]Centre d'hydrogéologie et de géothermie, Université de Neuchâtel, Neuchâtel 2000, Switzerland.

Corresponding author: Diana Rodríguez-Fernández (diana.rodriguez@ub.edu)

Journal: Chemosphere

Figures: 4

Tables: 2

Published in **Chemosphere** 206 (2018) 447-456, <https://doi.org/10.1016/j.chemosphere.2018.05.036>

Abstract

A dual element C-Cl isotopic study was performed for assessing chlorinated methanes (CMs) abiotic transformation reactions mediated by iron minerals and Fe(0) to further distinguish them in natural attenuation monitoring or when applying remediation strategies in polluted sites. Isotope fractionation was investigated during carbon tetrachloride (CT) and chloroform (CF) degradation in anoxic batch experiments with Fe(0), with FeCl₂(aq), and with Fe-bearing minerals (magnetite, Mag and pyrite, Py) amended with FeCl₂(aq), at two different pH values (7 and 12) representative of field and remediation conditions. At pH 7, only CT batches with Fe(0) and Py underwent degradation and CF accumulation evidenced hydrogenolysis. With Py, thiolytic reduction was revealed by CS₂ yield and is a likely reason for different Λ value ($\Delta\delta^{13}\text{C}/\Delta\delta^{37}\text{Cl}$) comparing with Fe(0) experiments at pH 7 (2.9 ± 0.5 and 6.1 ± 0.5 , respectively). At pH 12, all CT experiments showed degradation to CF, again with significant differences in Λ values between Fe(0) (5.8 ± 0.4) and Fe-bearing minerals (Mag, 2 ± 1 , and Py, 3.7 ± 0.9), probably evidencing other parallel pathways (hydrolytic and thiolytic reduction). Variation of pH did not significantly affect the Λ values of CT degradation by Fe(0) nor Py.

CF degradation by Fe(0) at pH 12 showed a Λ (8 ± 1) similar to that reported at pH 7 (8 ± 2), suggesting CF hydrogenolysis as the main reaction and that CF alkaline hydrolysis (13.0 ± 0.8) was negligible.

Our data establish a base for discerning the predominant or combined pathways of CMs natural attenuation or for assessing the effectiveness of remediation strategies using recycled minerals or Fe(0).

keywords (6 words): CSIA, carbon tetrachloride, chloroform, pyrite, Fe(0), degradation pathways

1. Introduction

Chloroform (CF, CHCl_3) and carbon tetrachloride (CT, CCl_4) are chlorinated volatile organic compounds (VOCs) from the group of chlorinated methanes (CMs). Both are toxic and predicted to be carcinogenic substances (IARC, 1999). They are found in groundwater as a consequence of releases from chemical manufacturing processes or accidental spills (Zogorski et al., 2006), although CF can also be naturally formed (Cappelletti et al., 2012; Hunkeler et al., 2012; Breider et al., 2013).

Abiotic CMs degradation in groundwater mainly proceeds under anoxic conditions. The main CT degradation pathway is hydrogenolysis to CF, although CT reduction followed by hydrolytic or thiolytic substitution of dechlorinated intermediates to CO, CO_2 or CS_2 is also possible (He et al., 2015). Abiotic CF degradation processes under anoxic conditions include hydrogenolysis to DCM and reductive elimination to CH_4 (Song and Carraway, 2006; He et al., 2015). Bioremediation strategies for CMs are scarce (Penny et al., 2010; Cappelletti et al., 2012; Koenig et al., 2015). Thus, although both compounds can be biotically (Penny et al., 2010; Cappelletti et al., 2012) or abiotically degraded, they are considered recalcitrant compounds requiring targeted remediation strategies in groundwater.

In situ chemical oxidation is not an effective treatment for CT and CF due to the highly oxidized state of carbon (Huang et al., 2005; Huling and Pivetz, 2006). Alkaline hydrolysis (AH) has been studied for CF at laboratory and field scale as a new and effective remediation strategy (Torrentó et al., 2014) but CT hydrolysis is pH independent and extremely slow (Jeffers et al., 1989). Fortunately, zero-valent metals and Fe-bearing minerals have proven to mediate the transformation of CF and CT at laboratory scale (e.g. Matheson and Tratnyek, 1994; Támara and Butler, 2004; Feng and Lim, 2005; Zwank et al., 2005; He et al., 2015; Lee et al., 2015). Fe(0) has been commonly used in permeable reactive barriers (PRBs) since it is a strong reducing agent, cheaper and less harmful than other zero-valent metals (Vodyanitskii, 2014). Micro-sized Fe(0) has been used in long-functioning PRBs, while nano-sized Fe(0) injections have been recently used to renew PRBs in highly polluted sites (Obiri-Nyarko et al., 2014). Some minerals such as magnetite (Fe_3O_4 , Mag hereafter) can be formed in Fe(0) PRBs reducing their efficiency (Vodyanitskii, 2014), while others, such as FeS, can promote CT degradation (Obiri-Nyarko et al., 2014). Since long-term evolution of PRBs is still not fully understood (Obiri-Nyarko et al., 2014) and Fe-bearing minerals such as pyrite (FeS_2 , Py hereafter), green rusts or Mag are naturally ubiquitous in anoxic aquifers and/or in transition zones (Ferrey et al., 2004; Scheutz et al., 2011), it is interesting to assess their influence on CMs degradation.

Detection of CMs natural attenuation or monitoring of the above-mentioned remediation strategies can be challenging when relying on only by-products, since these daughter products can be further degraded, are difficult to quantify in the field (e.g. gases), could come from other parent compounds or stem from a secondary source (i.e. CF). In such cases, compound specific isotope analysis (CSIA) has been developed and matured into a widely applied method allowing the investigation of VOCs transformation reactions and the associated isotopic fractionation values (ϵ) (Renpenning and Nijenhuis, 2016). The occurrence of limiting steps prior to the reaction step that mask the real magnitude of the ϵ has been shown when mineral phases are involved in abiotic degradation processes (Elsner et al., 2007). Controlled laboratory studies are thus required to confine the ranges of possible ϵ values and determine conservative estimates of quantification of CMs degradation extent in the field. The concept of dual element (C-Cl) isotope plots featuring slopes ($\Lambda = \Delta\delta^{13}\text{C}/\Delta\delta^{37}\text{Cl}$) that are characteristic of different reaction mechanism, holds promise to provide information on the manner and order of chemical bond cleavage for organohalides (Nijenhuis et al., 2016) and this, in turn, may help to distinguish potential competing processes and to assess their individual effectiveness as field remediation strategies (Van Breukelen, 2007). Although some abiotic Λ values for CF were recently published (Heckel et al., 2017a; Torrentó et al., 2017), neither Λ for CT abiotic reactions nor field demonstrations are available.

In a multiple-compound polluted site in Òdena (Catalonia) (Palau et al., 2014), shifts in carbon isotopic composition of CF were attributed to AH (Torrentó et al., 2014) since alkaline conditions (pH ~12) were generated in recharge water concrete-based interception trenches. In contrast, detected shifts in the carbon isotopic composition of CT could not be explained by AH but here, reduction by Fe-bearing materials from the construction wastes used in the trenches could have played an important role (Torrentó et al., 2014). The presence of surficial iron patinas growths and of variable iron amounts in concrete-based aggregates obtained from one of the boreholes was confirmed by Scanning Electron Microscopy with X-ray microanalysis (SEM-EDS) and X-ray fluorescence (XRF) (data not published), but specific mineral phases are still under study.

In order to close this knowledge gap on isotopic data of abiotic CMs reactions and, therefore, to allow better field interpretations such as in the case of Òdena, this study aims at providing dual element isotope data on abiotic degradation of CT and CF by Fe(0) and Fe-bearing minerals with $\text{FeCl}_2(\text{aq})$ under anoxic conditions at pH 7 and 12. Characterization is based on monitoring the carbon and chloride isotopic composition ($\delta^{13}\text{C}$ and $\delta^{37}\text{Cl}$) of CF and CT, as well as on detecting volatile dissolved by-products to

identify the existence of parallel reaction pathways. Nano-sized Fe(0) was used for CT experiments because it is more reactive than micro-sized Fe(0) (Song and Carraway, 2006). CF experiments at pH 12 were performed with milli-sized Fe(0) to compare the pH effect with published pH 7 experiments (Torrentó et al., 2017). Py and Mag were chosen as Fe-bearing minerals because they involve different potential redox species for reaction with CMs (Fe(II), and S_2^{2-} in Py, according to Kriegman-King and Reinhard, 1994) and represent widespread oxidation products of Fe(0) in PRBs (He et al., 2015) and mining or industrial wastes, which are potential recyclable materials for remediation.

2. Materials and methods

2.1. Experimental setup

Experiments were prepared in an anaerobic chamber and performed in 42 mL VOA/EPA glass vials capped with PTFE-coated rubber stoppers and plastic screw caps. A summary of experiment nomenclature, amendments and concentrations, incubation parameters representative of typical environmental conditions and performed analyses is provided in Table 1, together with data from already published CF experiments with milli-sized Fe(0) at pH 7 (Torrentó et al., 2017) for the sake of comparison. After the addition of the solid phase, vials were completely filled with buffered aqueous solution (at pH 7 or 12) without headspace, except for CT experiments with nano-sized Fe(0), for which the vials contained 21 mL liquid phase and 21 mL gas phase. For Mag and Py batches, $FeCl_2(aq)$ was also added to the buffered solution to better mimic field conditions, and because it is thought that CT degradation reactions can be surface-mediated by Fe(II) sorbed to solid phases (Scherer et al., 1998; Amonette et al., 2000; Pecher et al., 2002; Elsner et al., 2004). Bottles with 0.6 mM of $FeCl_2(aq)$ and without Fe-minerals (named as 'aq') were prepared as reactive controls for the potential of $FeCl_2(aq)$ for CMs degradation. Controls (CO) with only buffered solution at the corresponding pH were prepared to observe losses or effects of the pH itself on CF transformation. The reaction started with the addition of pollutant pure phase to reach the initial theoretical concentration. Vials were placed in horizontal shakers at room temperature until sampling. Replicates (n vials) were prepared for each experiment and reaction vials were sacrificed at appropriate time intervals. The CT experiments with nano-sized Fe(0) were conducted in triplicate and headspace samples were taken from each single vial at appropriate time intervals. Concentration and C and Cl isotope ratios of parent compounds and potential by-products were monitored over time. The used analytical methods are included in Table 1.

Although Eh could not be monitored, it would be assumed below 0 V, postulated as the boundary for anoxic conditions (Morris et al., 2003; Hosono et al., 2011). At these Eh conditions, Fe(0) (and Py to a lesser extent) is not stable at pH 7 neither 12 (Fig.S1). Thermodynamically, Fe(0) oxidation should occur and electron release should be expected. More details about chemicals, minerals and Fe(0) preparation and characterization, sampling, samples preservation and analytical methods are available in the Supplementary Information (SI).

1 Table 1. Summary of performed experiments nomenclature, conditions, procedure and analyses. The equipment used for each analysis is specified. n.u.= not used in the experiment, n.a.=not analyzed.

| Pollutant | pH | Name | Pollutant concentration (mM) | Fe(0)/mineral loading (m ² /L) | FeCl ₂ (mM) | n vials | Incubation temperature (°C) | Incubation time (days) | Shaker | By-products analyses | δ ¹³ C analyses of parent compounds and by-products | δ ³⁷ Cl analyses of parent compounds | Ref. | | | | | | | |
|-----------|----------|-----------|------------------------------|---|------------------------|-----------|------------------------------------|--|------------------------------------|--|---|---|---|------------------------------------|--|---|---|--|---|------------------------------------|
| CT | 7 | CT_Fe_7 | 2.6 | 28 | n.u. | 1 | 25±2 | 0.1 | Horizontal ^a 300 rpm | VOCs HS-GC-qMS-1 ^d as described in Heckel et al. (2017b) | HS-GC-IRMS-2 ^d as described in Cretnik et al. (2013) | HS-GC-IRMS-2 ^d as described in Heckel et al. (2017b) | This study | | | | | | | |
| | 12 | CT_Fe_12 | | | | 1 | 25±2 | 0.1 | Horizontal ^a 300 rpm | | | | | | | | | | | |
| | 7 | CT_aq_7 | 0.3 | n.u. | 0.6 | 9 | 17.4±0.3* | 11 | Horizontal ^b 100 rpm | VOCs, CS ₂ HS-GC-MS ^e as described in Torrentó et al. (2017) | SPME-HS-GC- IRMS-1 ^e as described in Martín-González et al. (2015) | HS-GC-qMS-2 ^f as described in Heckel et al. (2017b) (n.a. for CT_Mag_7) | | | | | | | | |
| | 12 | CT_aq_12 | | | | 11 | 19.2±0.4* | 9 | | | | | | | | | | | | |
| | 7 | CT_Mag_7 | | | | 5 | 20±2* | 0.9 | | | | | | | | | | | | |
| | 12 | CT_Mag_12 | 7 | 15±3* | 11 | 0.6 | 20 | 20±2* | | | | | | 9 | | | | | | |
| | 7 | CT_Py_7 | 0.3 | 17 | 0.6 | 20 | 18.7±0.3* | 4 | | | | | | Horizontal ^b 100 rpm | VOCs, CS ₂ HS-GC-MS ^e as described in Torrentó et al. (2017) | SPME-HS-GC- IRMS-1 ^e as described in Martín-González et al. (2015) | HS-GC-qMS-2 ^f as described in Heckel et al. (2017b) (n.a. for CT_Mag_7) | | | |
| | 12 | CT_Mag_12 | | | | 19 | 20±1* | 7 | | | | | | | | | | | | |
| 7 | CT_Py_7 | 20 | | | | 20.2±0.1* | 1 | | | | | | | | | | | | | |
| 12 | CT_Py_12 | 59 | 0.6 | 19 | 20±1* | 7 | Horizontal ^b 100 rpm | VOCs, CS ₂ HS-GC-MS ^e as described in Torrentó et al. (2014) | | | | | SPME-HS-GC- IRMS-1 ^e as described in Martín-González et al. (2015) | | | | | HS-GC-qMS-2 ^f as described in Heckel et al. (2017b) n.a. HS-GC-qMS-2 ^f as described in Heckel et al. (2017b) n.a. | | |
| 7 | CF_CO_7 | 0.9 | n.u. | n.u. | 6 | 25±2 | | | 2 | Horizontal ^c 200 rpm | VOCs HS-GC-TOF- MS ^d as described in Torrentó et al. (2017) | HS-GC-IRMS-2 ^d as described in Heckel et al. (2017b) | | | | | | | Torrentó et al. (2017) | |
| 12 | CF_CO_12 | 0.4 | n.u. | n.u. | 12 | 25±2 | | | 9 | | | | | | | | | | This study | |
| CF | 7 | CF_Fe_7 | 0.9 | 77 | n.u. | 20 | | | 25±2 | 2 | Horizontal ^c 200 rpm | VOCs HS-GC-TOF- MS ^d as described in Torrentó et al. (2017) | | | | | | | HS-GC-IRMS-2 ^d as described in Heckel et al. (2017b) | Torrentó et al. (2017) |
| | 12 | CF_Fe_12 | | | | 20 | | | 25±2 | 9 | | | | | | | | | | Horizontal ^b 100 rpm |
| | 7 | CF_aq_7 | 0.4 | n.u. | 0.6 | 9 | | | 17.4±0.5* | 8 | | | | | | | | | | |
| | 12 | CF_aq_12 | | | | 10 | | | 17.2±0.7* | 23 | | | | | | | | | | |
| | 7 | CF_Mag_7 | | | | 17 | | | 0.6 | 19 | 17.0±0.5* | 21 | | | | | | | | |
| | 12 | CF_Mag_12 | 20 | 17.0±0.6* | 23 | | | | | | | | | | | | | | | |
| | 7 | CF_Py_7 | 0.4 | 59 | 0.6 | 19 | 18±1* | 21 | Horizontal ^b 100 rpm | VOCs, CS ₂ HS-GC-MS ^e as described in Torrentó et al. (2014) | SPME-HS-GC- IRMS-1 ^e as described in Martín-González et al. (2015) | HS-GC-qMS-2 ^f as described in Heckel et al. (2017b) n.a. | | | | | | | | |
| | 12 | CF_Py_12 | | | | 20 | 17.4±0.5* | 22 | | | | | | | | | | | | |

2 ^aR1000 ROTH; ^bDenlay Instruments LTD n°941157; ^cIKA KS 260 BASIC; ^din Institute of Groundwater Ecology of *Helmholtz Zentrum (München)*; ^ein *Universitat de Barcelona*; ^fin *Université de Neuchâtel*. Equipment
3 abbreviations correspond to headspace (HS)-gas chromatography (GC)- mass spectrometry (MS); HS-GC coupled to a time-of-flight (TOF) MS; GC quadrupole MS (GC-qMS); GC coupled to an isotope ratio mass
4 spectrometer (GC-IRMS). *Spot measurement when sampling.

5 **3. Results and discussion**

6 In the following sections, isotope results for CF and CT degradation by the Fe(0), Mag, Py and FeCl₂(aq)
7 are presented (Table 2) and compared with literature data. Concentrations were lower than expected in
8 some experiments probably due to sorption on non-reactive sites of initial or newly formed solid phases
9 as observed by other authors (Burriss et al., 1995,1998; Kim and Carraway, 2000; Song and Carraway,
10 2006). pH was constant for all experiments (SD<0.5) except for CF_Mag_12, CF_Py_12, CT_aq_7,
11 CT_Mag_7 (Fig. S2) where higher fluctuations might be attributable to iron corrosion processes and
12 Fe(OH)₃(am) formation.

13

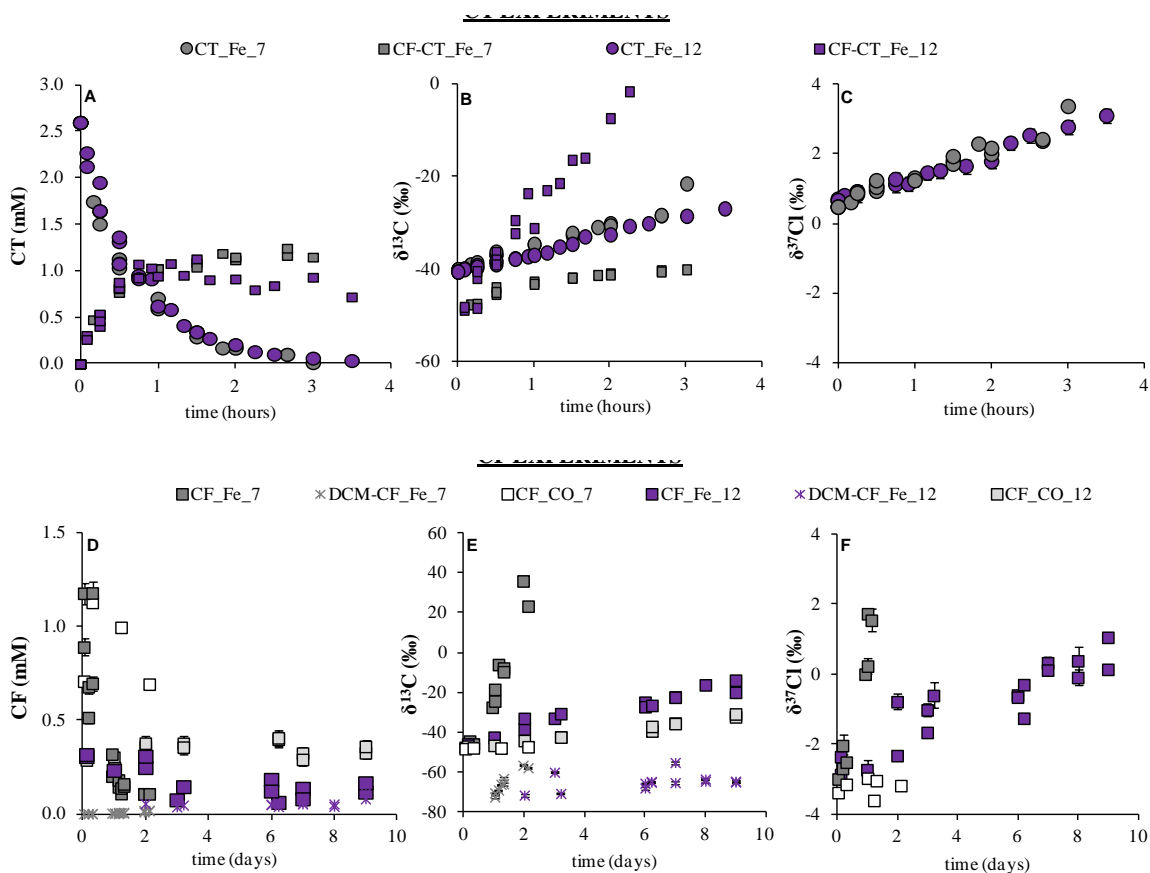
14 Table 2. Summary of isotope results, identified by-products and hypothesized degradation pathways. Uncertainty of ϵ , AKIE and Λ
 15 ($\Delta\delta^{13}\text{C}/\Delta\delta^{37}\text{Cl}$) values corresponds to the 95% confidence intervals. AKIEs were calculated assuming C-Cl bond cleavage in the
 16 first rate-limiting reaction step. AKIE_C values for CT and CF were calculated with $z=x=n=1$ and AKIE_{Cl} values with $z=x=n=4$ for
 17 CT and of $z=x=n=3$ for CF (Calculations in SI). Question marks indicate hypothesized pathways not proved in this research.

| Experiment | By-products* | ϵ (%) | AKIE | Λ | Removal (%) | Proposed pathway |
|----------------------|---------------------|---|--|------------------------------------|-------------|--|
| CT_Fe_7 | CF | $\epsilon_C = -3.7 \pm 0.1$ $R^2 = 0.995$ $\epsilon_{\text{Cl}} = -0.58 \pm 0.04$ $R^2 = 0.98$ | $\text{AKIE}_C = 1.0037 \pm 0.0001$ $\text{AKIE}_{\text{Cl}} = 1.00233 \pm 0.00004$ | 6.1 ± 0.5 $R^2 = 0.98$ | 99 | Hydrogenolysis |
| CT_Fe_12 | CF | $\epsilon_C = -3.4 \pm 0.1$ $R^2 = 0.993$ $\epsilon_{\text{Cl}} = -0.55 \pm 0.03$ $R^2 = 0.98$ | $\text{AKIE}_C = 1.0034 \pm 0.0001$ $\text{AKIE}_{\text{Cl}} = 1.00220 \pm 0.00003$ | 5.8 ± 0.4 $R^2 = 0.98$ | 99 | Hydrogenolysis |
| CT_aq_7 | n.d. | no degradation | | | | |
| CT_aq_12 | CF | $\epsilon_C = -3 \pm 3$ $R^2 = 0.50$ | $\text{AKIE}_C = 1.003 \pm 0.003$ | High confidence interval | 87 | Hydrogenolysis |
| CT_Mag_7 | n.d. | no degradation | | | | |
| CT_Mag_12 | CF | $\epsilon_C = -2 \pm 1$ $R^2 = 0.70$ $\epsilon_{\text{Cl}} = -0.8 \pm 0.2$ $R^2 = 0.93$ | $\text{AKIE}_C = 1.002 \pm 0.001$ $\text{AKIE}_{\text{Cl}} = 1.0032 \pm 0.0002$ | 2 ± 1 $R^2 = 0.65$ | 98 | Hydrogenolysis \pm hydrolytic reduction? |
| CT_Py_7 | CF, CS ₂ | $\epsilon_C = -5 \pm 2$ $R^2 = 0.70$ $\epsilon_{\text{Cl}} = -1.5 \pm 0.4$ $R^2 = 0.8$ | $\text{AKIE}_C = 1.005 \pm 0.002$ $\text{AKIE}_{\text{Cl}} = 1.0060 \pm 0.0004$ | 2.9 ± 0.5 $R^2 = 0.9$ | 99 | Hydrogenolysis and thiolytic reduction |
| CT_Py_12 | CF, CS ₂ | $\epsilon_C = -4 \pm 1$ $R^2 = 0.87$ $\epsilon_{\text{Cl}} = -0.9 \pm 0.4$ $R^2 = 0.84$ | $\text{AKIE}_C = 1.004 \pm 0.001$ $\text{AKIE}_{\text{Cl}} = 1.0036 \pm 0.0004$ | 3.7 ± 0.9 $R^2 = 0.93$ | 99 | Hydrogenolysis and thiolytic reduction |
| CF_CO_7 | n.d. | no degradation | | | | |
| CF_CO_12 | n.d. | n.c. | n.c. | | | Partly by AH \pm reductive elimination? |
| CF_Fe_7 ^a | DCM | $\epsilon_C = -33 \pm 11$ $R^2 = 0.82$ $\epsilon_{\text{Cl}} = -3 \pm 1$ $R^2 = 0.85$ | $\text{AKIE}_C = 1.034 \pm 0.012$ $\text{AKIE}_{\text{Cl}} = 1.008 \pm 0.001$ | 8 ± 2 $R^2 = 0.93$ | 84 | Hydrogenolysis \pm reductive elimination? |
| CF_Fe_12 | DCM | $\epsilon_C = -20 \pm 9$ $R^2 = 0.62$ $\epsilon_{\text{Cl}} = -2 \pm 1$ $R^2 = 0.64$ | $\text{AKIE}_C = 1.020 \pm 0.009$ $\text{AKIE}_{\text{Cl}} = 1.006 \pm 0.001$ | 8 ± 1 $R^2 = 0.92$ | 85 | Hydrogenolysis \pm reductive elimination? |
| CF_aq_7 | n.d. | no degradation | | | | |
| CF_aq_12 | n.d. | $\epsilon_C = -16 \pm 13$ $R^2 = 0.70$ | $\text{AKIE}_C = 1.02 \pm 0.01$ | $\delta^{37}\text{Cl}$ values n.a. | 60 | Partly by AH \pm reductive elimination? |
| CF_Mag_7 | n.d. | no degradation | | | | |
| CF_Mag_12 | n.d. | $\epsilon_C = -16 \pm 9$ $R^2 = 0.65$ | $\text{AKIE}_C = 1.016 \pm 0.009$ | $\delta^{37}\text{Cl}$ values n.a. | 80 | Partly by AH \pm reductive elimination? |
| CF_Py_7 | n.d. | no degradation | | | | |
| CF_Py_12 | DCM | $\epsilon_C = -20 \pm 7$ $R^2 = 0.85$ | $\text{AKIE}_C = 1.020 \pm 0.007$ | $\delta^{37}\text{Cl}$ values n.a. | 62 | Hydrogenolysis \pm reductive elimination and partly by AH? |

18 ^aFrom Torrentó et al. (2017). ^{*}Potential gas by-products such as CO, CO₂, CH₄ or formate were not analyzed. n.c.= not calculated,
 19 n.d.=not detected; n.a.=not analyzed
 20

21 **3.1. Degradation study by Fe(0)**

22 At both pH 7 and 12, CT concentration decrease below the detection limit in experiments with nano-sized
 23 Fe(0) was achieved before 4h (Fig. 1A) and followed a pseudo-first-order kinetic law with rate constant
 24 values k_{SA} of $(4.9\pm 0.6)\times 10^{-2}$ and $(4.4\pm 0.1)\times 10^{-2}$ Lm⁻²h⁻¹, respectively (Table S1). pH effect on k_{SA} was
 25 minimal as expected by thermodynamics, since E⁰ of Fe(0) transformation to Fe(II) does not depend on
 26 pH.



27
 28 Fig. 1. Concentration (A, D), carbon (B, E) and chlorine (C, F) isotope composition ($\delta^{13}C$ and $\delta^{37}Cl$, ‰) over time in the CT (upper
 29 panels) and CF (lower panels) experiments at pH 7 and 12 with Fe(0) and control CF experiments (CO). CF_Fe_7 and CF_CO_7
 30 data from Torrentó et al. (2017), and concentration and $\delta^{13}C$ evolution of CF and DCM as CT and CF by-products, respectively, are
 31 also shown. $\delta^{37}Cl$ data of by-products are not available. Error bars are smaller than symbols.

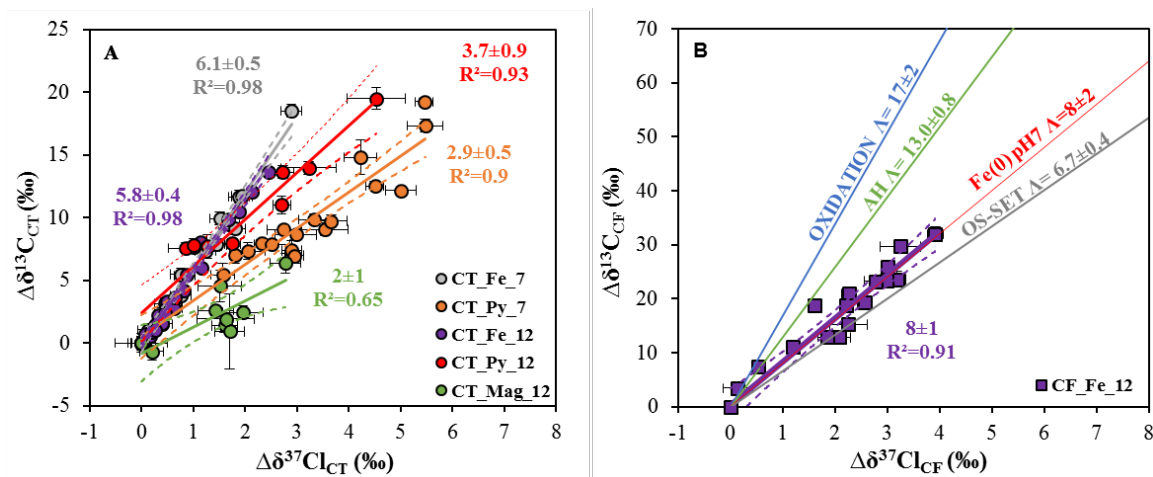
32
 33 Significant shifts in $\delta^{13}C_{CT}$ and $\delta^{37}Cl_{CT}$ were detected after 99.4% and 98.6% of CT removal at pH 7 and
 34 12, respectively (Fig. 1B and C), resulting in very similar $\epsilon_{C_{CT}}$ (-3.7 ± 0.1 , $R^2=0.995$ and -3.4 ± 0.1 ,
 35 $R^2=0.993$, respectively, see Eq. S4 and Fig. S3) and $\epsilon_{Cl_{CT}}$ values (-0.58 ± 0.04 , $R^2=0.98$ and -0.55 ± 0.03 ,
 36 $R^2=0.98$, respectively). Calculated AKIE_C values (Eq. S5) were therefore also similar at pH 7
 37 (1.0037 ± 0.0001) and 12 (1.0034 ± 0.0001) as for AKIE_{Cl} values (1.0023 ± 0.0004 and 1.00220 ± 0.00003 ,

38 respectively) (Table S2). These similarities regardless of pH confirmed that pH affects primarily
39 intermediate [$\cdot\text{CCl}_3$] radical reactions rather than the initial rate-limiting step (Zwank et al., 2005). AKIEs
40 values were below 50% of the Streitwieser limit for a C-Cl bond cleavage ($\text{KIE}_\text{C}=1.057$, $\text{KIE}_\text{Cl}=1.013$)
41 (Elsner et al., 2005) and also below all reported values for abiotic and biotic reductive dechlorination of
42 chlorinated compounds (Table S2), indicating significant mass transfer masking effects. CT is rapidly
43 reduced when contacting a strong reducing agent like Fe(0) and, thus, the rate-limiting step of the reaction
44 might be the diffusion of CT through the solution to the Fe(0) surface rather than the C-Cl bond cleavage
45 (Arnold et al., 1999). In our experiments, this diffusion control could have been enhanced by the low
46 concentration of CT (2.6 mM) compared to Fe(0) loading (28 m^2/L), but further research would be
47 needed to confirm this hypothesis.

48 The use of HEPES in the pH 7 experiments might constrain exact quantitative by-product distribution as
49 it appears to alter by-product formation acting as possible $\text{H}\cdot$ radical donor and favoring CF formation
50 (Elsner et al., 2004; Danielsen et al., 2005). However, by-product distribution study was not the aim of
51 this work and by-products different from VOCs such as CH_4 , CO , CO_2 , (Lien and Zhang, 1999; Choe et
52 al., 2001; Song and Carraway, 2006) were not analyzed. CF (45-56%) and DCM (up to 0.3% of initial
53 CT) were detected as by-products at pH 7 and 12, after 99% of CT degradation, similarly to what was
54 reported previously (Helland et al., 1995; Támara and Butler, 2004; Song and Carraway, 2006; Lien et al.,
55 2007; Feng et al., 2008), which confirms CT and CF hydrogenolysis. Isotopic mass balances showed a
56 maximum $\Delta\delta^{13}\text{C}_{\text{SUM}}$ (defined as final $\delta^{13}\text{C}_{\text{SUM}}$, Eq. S6, with respect to initial $\delta^{13}\text{C}_{\text{SUM}}$ considering, CT and
57 by-product CF data) of only +1.5‰ at pH 7, compared to +35‰ at pH 12. Thus, at pH 7, CF degradation
58 to other by-product different from DCM was insignificant in the present experimental conditions and
59 duration (3.5 hours). At pH 12, however, important further CF degradation (and a possible formation of
60 other CT by-products) was evidenced by $\Delta\delta^{13}\text{C}_{\text{SUM}}$, $\Delta\delta^{13}\text{C}$ and more enriched $\delta^{13}\text{C}_{\text{CF}}$ values than those
61 $\delta^{13}\text{C}_{\text{CT}}$ values of the parental CT (Fig. 1B).

62 As carbon and chlorine CT isotope fractionation is affected to the same extent by the above-mentioned
63 masking effects, in a C-Cl dual plot these effects cancel out. As shown in Fig. 2A, Λ values obtained at
64 pH 7 and 12 are similar (6.1 ± 0.5 , $R^2=0.98$ and 5.8 ± 0.4 , $R^2=0.98$, respectively), and indicative of CT
65 hydrogenolysis attending to CF formation. The above-mentioned closed mass balances in CT_Fe_7 and
66 the similar Λ at both pH revealed that CT hydrogenolysis by Fe(0) might also be the main pathway at pH
67 12. Moreover, if CT parallel pathways occur at pH 12, they should involve one C-Cl bond cleavage as

68 hydrogenolysis does (Scheme S1). The obtained Λ values for CT degradation by Fe(0) show no
 69 statistically significant difference (with statistical significance at the $p < 0.05$ level, ANCOVA, $p = 0.8$) to
 70 that reported for biotically-mediated CT anaerobic degradation detected in field-derived microcosms
 71 (6.1 ± 0.5) (Rodríguez-Fernández et al., 2018).



72
 73 Fig. 2. Dual C-Cl isotope plot for CT (A) and CF (B) abiotic experiments. Same coloured solid and dashed lines correspond to linear
 74 regressions of the data sets of this study and 95% CI, respectively. Error bars show uncertainty in duplicate isotope measurements
 75 except for CT_Fe_7 and CT_Fe_12 experiments, where 0.5‰ and 0.2‰ were considered for $\delta^{13}\text{C}$ and $\delta^{37}\text{Cl}$, respectively. In some
 76 cases, error bars are smaller than symbols. Solid slopes in B correspond to CF abiotic degradation reference systems: oxidation by
 77 thermally-activated persulfate (blue), alkaline hydrolysis, AH (green), dechlorination by Fe(0) at pH 7 (red) (Torrentó et al., 2017)
 78 and reductive outer-sphere electron transfer by CO_2 radical anions, OS-SET (grey) (Heckel et al., 2017a).

79
 80 The CF_Fe_12 experiments were carried out to complement existing data at pH 7 with milli-sized Fe(0)
 81 (Torrentó et al., 2017) (CF_Fe_7 in Table 1) and to provide, thereby, a more comprehensive picture of
 82 isotope effects in CF reduction by Fe(0). The corresponding control experiment without Fe(0)
 83 (CF_CO_12) showed certain variation in CF concentration (Fig. 1D) and although no VOCs by-products
 84 were detected, a significant $\delta^{13}\text{C}_{\text{CF}}$ shift of +17.6‰ was shown after 9 days (Fig. 1E). Since no isotopic
 85 changes occurred in previously reported CF_CO_7 (Torrentó et al. 2017), the results of CF_CO_12
 86 experiment suggest that CF was degraded by AH. Assuming this was the only degradation fractionation
 87 process, the CF transformation extent by AH in CF_CO_12 was estimated to be $27 \pm 7\%$ using Eq. S7 and
 88 the ϵ_{C} of -57 ± 5 ‰ obtained by Torrentó et al. (2017). This extent of degradation fits well with the
 89 reported CF hydrolysis rates (Torrentó et al., 2014; 2017).

90 In the CF_Fe_12 experiment, CF degradation was also evidenced. CF concentration decreased with some
 91 fluctuations (Fig. 1D) causing poor correlation in rate constant k_{SA} ($(1.4 \pm 0.6) \times 10^{-3} \text{ Lm}^{-2}\text{d}^{-1}$, $R^2 = 0.67$,

92 Table S1) and ϵ calculations ($\epsilon_{\text{CF}}=-20\pm 9$ $R^2=0.62$ and $\epsilon_{\text{Cl}_{\text{CF}}}=-2\pm 1$, $R^2=0.64$) (Fig. S4). Hence,
93 comparison to CF_Fe_7 and literature data was based on evaluation of Λ values.

94 In this experiment, a moderated DCM accumulation was detected as by-product ($\leq 0.3\%$ yield after 9
95 days). This, together with the slower CF consumption in CF_Fe_12 compared to CF_Fe_7 (Fig. 1D),
96 could be explained by Fe(0) surface passivation due to Fe-oxyhydroxides precipitation, enhanced at
97 alkaline pH (Farrell et al., 2000; Támara and Butler, 2004). Low $\Delta\delta^{13}\text{C}_{\text{DCM}}$ was measured at pH 12
98 (+16‰ after 85% of CF removal) (Fig. 1E) similar to pH 7 (+15‰, after 87% of CF removal, Torrentó et
99 al., 2017). The $\Delta\delta^{13}\text{C}_{\text{SUM}}$ (taking into account CF and DCM data) at pH 12 was only around +10‰, which
100 might suggest an isotope-branching from CF or its intermediates (Zwank et al., 2005), that might have
101 produced the low DCM carbon isotope fractionation observed for both pH.

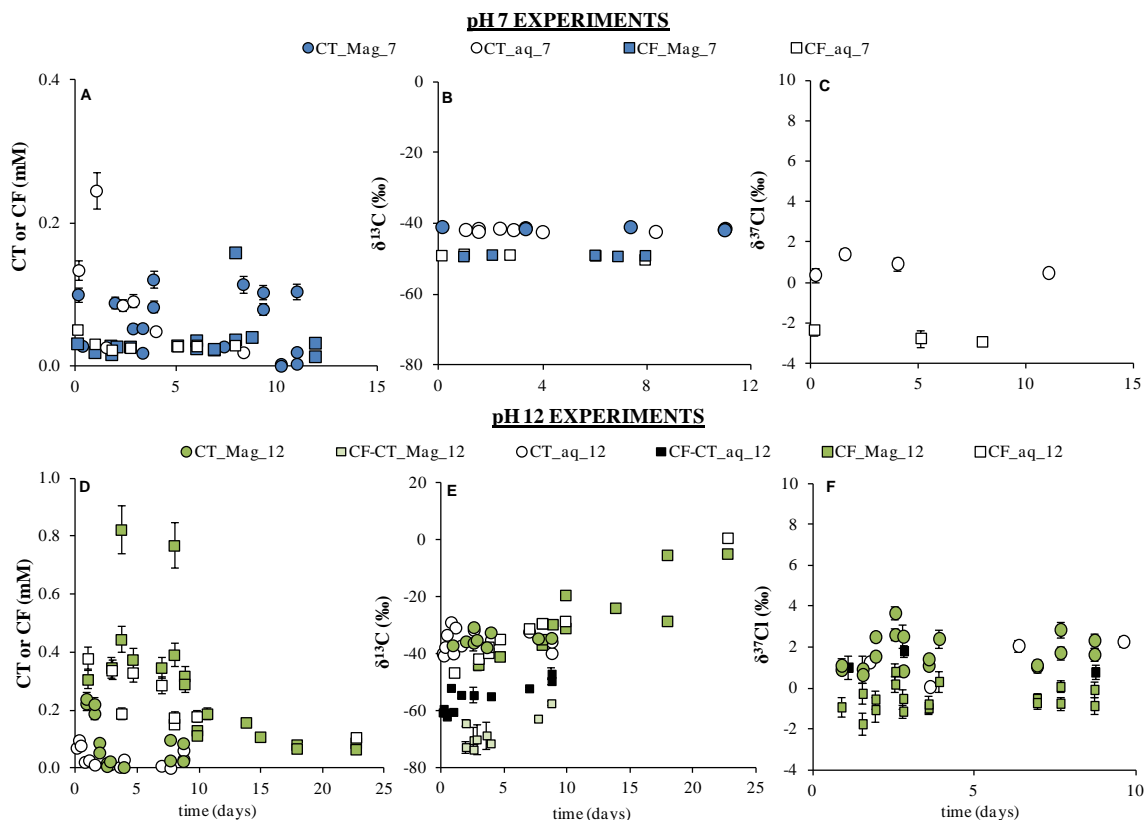
102 The Λ value for CF_Fe_12 was 8 ± 1 ($R^2=0.91$), not significantly different from that of Torrentó et al.
103 (2017) for CF_Fe_7 ($p=0.05065$) (Fig. 2B). Combining the data at pH 7 and 12, the Λ value is not
104 significantly different from that of CF reaction in model systems for outer-sphere single electron transfer
105 (OS-SET) ($p=0.1056$) (Heckel et al., 2017a), suggesting a concerted C-Cl bond cleavage, involving OS-
106 SET in the first rate-limiting step. For CF_Fe_7, Torrentó et al. (2017) postulated two parallel CF
107 dechlorination pathways (hydrogenolysis and reductive elimination) as reported for other CF reduction
108 studies with micro-sized Fe(0) (Matheson and Tratnyek, 1994; Feng and Lim, 2005; Song and Carraway,
109 2006). In the present experiments, CF reductive elimination related by-products (e.g. CH_4 , CO and
110 HCOO^-) were not analyzed, and thus, further conclusions are limited. The similar Λ values for Fe(0) are
111 far from the $\Lambda=13.0\pm 0.8$ for CF AH (Torrentó et al., 2017), indicating that AH in CF_Fe_12 was
112 negligible. Accordingly, negligible contribution of AH was evidenced by assessing the distribution (F) of
113 AH and dechlorination by Fe(0) to the total CF degradation following Van Breukelen (2007) and using
114 Eq (S8) and ϵ data from Torrentó et al. (2017).

115

116 **3.2. Degradation study by $\text{FeCl}_2(\text{aq})$ and Mag**

117 Despite concentration fluctuations (Fig. 3A), no significant $\delta^{13}\text{C}_{\text{CT}}$ shifts over time were observed in the
118 CT_aq_7 and CT_Mag_7 experiments ($-41.9\pm 0.5\%$, $n=9$ and $-41.4\pm 0.5\%$, $n=6$, respectively, Fig.3B) and
119 no VOCs by-products were detected. CT degradation therefore does not seem to occur in these
120 experiments. In fact, the analogous experiments with CF at pH 7 neither showed also significant changes
121 in $\delta^{13}\text{C}_{\text{CF}}$ ($-49.2\pm 0.2\%$, $n=5$, and $-49.0\pm 0.6\%$, $n=7$, for CF_Mag_7 and CF_aq_7 experiments,
122 respectively) (Fig.3B). This agrees with the decrease in the degradation efficiency of aged Fe(0) PRBs

123 when Mag is formed through corrosion (Vodyanitskii, 2014). However, CT degradation by Mag has been
 124 previously reported in the literature under different experimental conditions (Zwank et al., 2005; Hanoch
 125 et al., 2006; Maithreepala and Doong, 2007; Vikesland et al., 2007). Further discussion about this
 126 discrepancy can be found in the SI.



127
 128 Fig. 3. Concentration (A, D) and carbon (B, E) and chlorine (C, F) isotope composition ($\delta^{13}C$ and $\delta^{37}Cl$, ‰) over time in the CT and
 129 CF experiments at pH 7 (upper panels) and 12 (lower panels) with magnetite and $FeCl_2(aq)(Mag)$ and $FeCl_2(aq)$ alone (aq). Isotope
 130 data of by-products of each experiment are also shown and named as 'by-product-experiment name' to distinguish them from
 131 experiments where those compounds are parental compounds. In some cases, error bars are smaller than symbols.

132
 133 In contrast, at pH 12, CT degradation occurred and kinetics of CT_Mag_12 and CT_aq_12 followed a
 134 pseudo-first-order rate law with a k_{SA} of $(8 \pm 5) \times 10^{-2} Lm^{-2}d^{-1}$ and k' of $0.3 \pm 0.2 d^{-1}$, respectively (Table S3).
 135 CT degradation was confirmed by significant $\Delta\delta^{13}C_{CT}$ (Fig. 3E) and $\Delta\delta^{37}Cl_{CT}$ (Fig. 3F) after 87 and 98%
 136 CT removal in the CT_aq_12 and CT_Mag_12 experiments, respectively, obtaining $\epsilon_{CT} = -2 \pm 1\%$
 137 ($R^2 = 0.7$) and $\epsilon_{Cl_{CT}} = -0.8 \pm 0.2\%$ ($R^2 = 0.93$) for CT_Mag_12 (Fig. S6) and $\epsilon_{CT} = -2 \pm 3\%$ for CT_aq_12, but
 138 with poor linear regression ($R^2 = 0.5$) (Fig. S7). $AKIE_C$ (1.002 ± 0.0001) and $AKIE_{Cl}$ (1.0032 ± 0.0002)
 139 values of CT_Mag_12 were well below 50% of the Streitwieser limit for a C-Cl bond cleavage (Elsner et
 140 al., 2005) and also below the reported values for abiotic and biotic reductive dechlorination of chlorinated

141 compounds (Table S2), suggesting significant mass transfer masking effects as for Fe(0). A maximum CF
142 yield of +38% and +26% in CT_Mag_12 and CT_aq_12, respectively (Fig. S5), evidenced CT
143 hydrogenolysis. $\delta^{13}\text{C}$ enrichment in the produced CF was detected. To further study CF degradation,
144 analogous experiments with CF at pH 12 were performed and showed a CF concentration decrease to
145 values down to 0.2-0.1 mM after 23 days (Fig. 3D). Obtained pseudo-first-order rate constants had poor
146 correlation ($k'=(6\pm3)\times 10^{-2} \text{ d}^{-1}$, $R^2=0.6$, for CF_aq_12 and $k_{SA}=(6\pm2)\times 10^{-3} \text{ Lm}^{-2}\text{d}^{-1}$, $R^2=0.7$, for
147 CF_Mag_12, Table S3). In both experiments at pH 12, degradation was confirmed by $\delta^{13}\text{C}$ shifts
148 (Fig.3E). Comparing with the absence of CF degradation in the pH 7 analogous experiments, AH could
149 be assumed as the main degradation pathway in these experiments (Torrentó et al., 2017). However,
150 despite poor regression, the obtained values of EC_{CF} for CF_Mag_12 ($-16\pm 9\%$, $R^2=0.65$) and CF_aq_12
151 ($-16\pm 13\%$, $R^2=0.70$) (Fig. S6, S7) are in the range for CF reductive dechlorination studies (Table S2) and
152 far away from the reported values for CF AH at pH 12 ($-57\pm 5\%$) (Torrentó et al., 2017). These results
153 suggest the occurrence of additional parallel pathways (such as CF reductive elimination to CH_4)
154 (Scheme S1). Since nor CF Cl isotope ratios neither other non-chlorinated potential by-products were
155 measured in these experiments, further conclusions cannot be drawn.

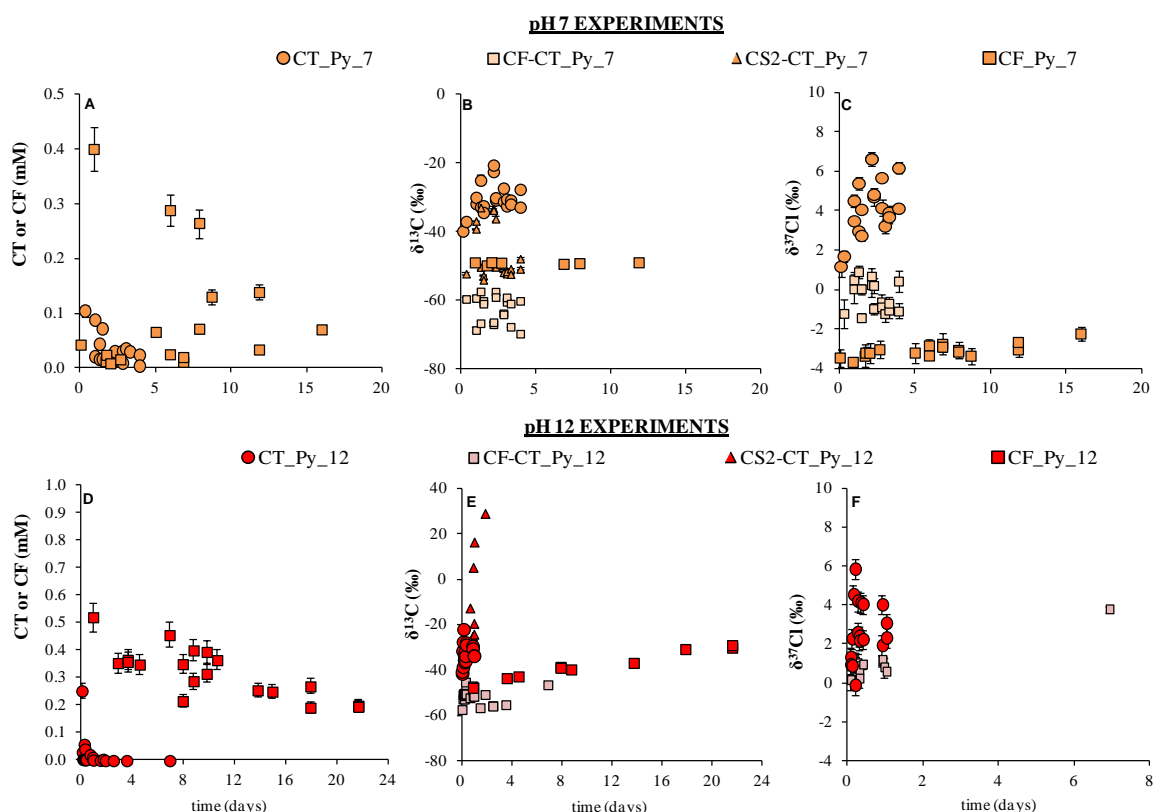
156 The calculated Λ value for CT_aq_12 (2 ± 3 , $R^2=0.67$) was discarded due to its wide confidence interval,
157 while that for CT_Mag_12 (2 ± 1 , $R^2=0.65$) (Fig. 2A) was, despite its poor linear regression, highly
158 statistically different ($p<0.0001$) from those of CT_Fe_7 and CT_Fe_12. It suggests that although CF was
159 formed as by-product in both Fe(0) and Mag CT experiments, parallel pathways other than
160 hydrogenolysis could have occurred in CT_Mag_12. Also, a different first rate-determining step between
161 reactions such as that producing CF or CO (hypothesized by-product by CT hydrolytic reduction
162 according to Danielsen and Hayes (2004) might have occurred. That case would question whether
163 branching in trichloromethyl free radical [$\cdot\text{CCl}_3$] or thrichlorocarbanion [$:\text{CCl}_3^-$] intermediates (Scheme
164 S1) were responsible for by-products distribution (Danielsen and Hayes, 2004; Elsner et al., 2004; Zwank
165 et al., 2005) because intermediates branching alone would have not affected CT isotope fractionation and
166 Λ would have been similar. Differences in Λ value might be also explained by a change in transition
167 states in mineral surfaces (Elsner et al., 2004).

168 The absence of CT degradation at pH 7 compared to pH 12, might be attributed to the control that pH
169 exerts on Mag reactivity (see SI for further discussion). Under our experimental conditions, CT
170 degradation by $\text{FeCl}_2(\text{aq})$ and Mag was only feasible under alkaline conditions. Although further field

171 research would be required, Mag might be responsible of $\delta^{13}\text{C}_{\text{CT}}$ fractionation detected in the alkaline
 172 trenches of the Òdena field site (Torrentó et al., 2014) given that Mag is an ubiquitous mineral,
 173 commonly present in construction wastes.

174 3.3. Degradation study by Py

175 CT concentrations in CT_Py_7 and CT_Py_12 decreased quickly, especially at pH 12 where they reached
 176 0.01 mM after 4h (Fig. 4A, D). Although poor correlated, degradation followed a pseudo-first-order rate
 177 law for CT_Py_7 ($k_{\text{SA}}=(1.6\pm 0.6)\times 10^{-2} \text{ Lm}^{-2}\text{d}^{-1}$, $R^2=0.72$) and CT_Py_12 ($(2\pm 1)\times 10^{-2} \text{ Lm}^{-2}\text{d}^{-1}$, $R^2=0.6$),
 178 (Table S3). CT degradation was confirmed at both pH by enrichment in ^{13}C and ^{37}Cl (Fig. 4). Calculated
 179 ϵ_{CT} and ϵ_{ClCT} values were $-5\pm 2\text{‰}$ ($R^2=0.7$) and $-1.5\pm 0.4\text{‰}$ ($R^2=0.8$), respectively for CT_Py_7 (Fig.
 180 S8), and $-4\pm 1\text{‰}$ ($R^2=0.87$) and $-0.9\pm 0.4\text{‰}$ ($R^2=0.84$), respectively for CT_Py_12 (Fig. S9).
 181 Corresponding AKIE_{C} (1.005 ± 0.002 and 1.004 ± 0.001 , respectively) and AKIE_{Cl} values (1.0060 ± 0.0004
 182 and 1.0036 ± 0.0004 , respectively) indicate significant mass transfer masking effects for the same reasons
 183 than for Fe(0) and Mag experiments. Poor correlation in CT_Py_7 might be linked to the low pH reached
 184 (4.7 ± 1.1 , Fig. S2) that might have caused changes in Py surface (Bonnissel-Gissinger et al., 1998)
 185 affecting CT degradation.

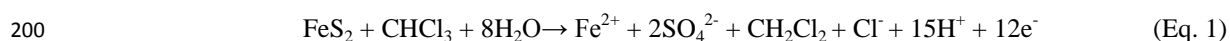


186 Fig. 4. Concentration (A, D) and carbon (B, E) and chlorine (C, F) isotope composition ($\delta^{13}\text{C}$ and $\delta^{37}\text{Cl}$, ‰) over time in the CT and
 187 CF experiments at pH 7 (upper panels) and 12 (lower panels) with pyrite (Py) and $\text{FeCl}_2(\text{aq})$. Isotope data of by-products of each
 188

189 experiment are also shown and named as 'by-product-experiment name' to distinguish them from experiments where those
190 compounds are parental compounds. In some cases, error bars are smaller than symbols.

191

192 In both experiments, the formation of by-products CF and CS₂ was observed (Fig. S5) agreeing with
193 literature (Kriegman-King and Reinhard, 1994; Devlin and Muller, 1999). Analogous experiments with
194 Py and CF as parent compound demonstrated no CF degradation at pH 7 ($\delta^{13}\text{C}_{\text{CF}}=-49.1\pm 0.3\%$, $\delta^{37}\text{Cl}_{\text{CF}}=-$
195 $3.1\pm 0.3\%$, $n=7$). At pH 12, however, CF degradation was evidenced by a clear CF concentration decrease
196 ($k_{\text{SA}}=(2\pm 1)\times 10^{-2}\text{ Lm}^{-2}\text{d}^{-1}$, $R^2=0.6$), a significant carbon isotope enrichment ($\epsilon_{\text{C}_{\text{CF}}}=-20\pm 7\%$, $R^2=0.85$) (Fig.
197 S9) and up to a 6% DCM yield (Fig. S5). Py oxidation at pH 12 by CF is an unknown process but, by
198 analogy to CT (Kriegman-King and Reinhard, 1992, 1994), it would follow Eq. (1), with an overall
199 reaction potential higher at pH 12 (0.7 V) than at pH 7 (0.5 V).



201 The accumulation of DCM (Fig. S5) suggests that hydrogenolysis together with AH might be responsible
202 for CF carbon isotope fractionation. Since $\delta^{37}\text{Cl}$ was not measured in this experiment, quantification of
203 each pathway following Eq. (S8) is not possible.

204 The detected CS₂ in the CT experiments with Py (Fig. S5) may form via aqueous or adsorbed HS⁻
205 (Kriegman-King and Reinhard, 1992) or via S₂²⁻ sites on Py surface acting as electron donor (Kriegman-
206 King and Reinhard, 1994). Despite fluctuations, shifts in $\delta^{13}\text{C}_{\text{CS}_2}$ values (Fig. 4B) and non-closed isotopic
207 mass balance calculations at pH 7 ($\delta^{13}\text{C}_{\text{SUM}}$ range from -44 to -59‰) might reveal further CS₂ degradation
208 since, as mentioned above, these shifts in $\delta^{13}\text{C}_{\text{SUM}}$ cannot be attributed to CF degradation. At pH 12, CS₂
209 degradation was confirmed by the much enriched $\delta^{13}\text{C}_{\text{CS}_2}$ values (+28.8‰) with respect to the initial
210 $\delta^{13}\text{C}_{\text{CT}}$ after 46h (Fig. 4E). CS₂ degradation might occur through hydrolysis mediated by hydroxide ions at
211 these alkaline conditions (11.8 ± 0.2). CS₂ alkaline hydrolysis has been proven at laboratory scale
212 (Svoronos and Bruno, 2002) with rate constants at 25 °C ranging between 10^{-4} and $10^{-3}\text{ M}^{-1}\text{s}^{-1}$, equivalent
213 to half-lives of 1-13 days at pH 11.8. According to literature (Peyton et al., 1976; Adewuyi and
214 Carmichael, 1987; Kriegman-King and Reinhard, 1992, 1994; McGeough et al., 2007), CS₂ is stable to
215 hydrolysis within the pH range of 4 to 10, suggesting Py mediation in the potentially occurring CS₂
216 degradation at pH 7, as Fe(0) involvement has also been reported (McGeough et al., 2007). Further
217 research is needed to clarify this point. In any case, it follows that the previously proposed CF:CS₂ mass
218 ratio for distinguishing CT transformations reactions (Devlin and Muller, 1999; Davis et al., 2003) is
219 inappropriate.

220 The obtained Λ values for CT_Py_7 (2.9 ± 0.5 , $R^2=0.9$) and CT_Py_12 experiments (3.7 ± 0.9 , $R^2=0.93$) are
221 similar to each other and to that of CT_Mag_12 ($p=0.2302$), but they are statistically different from that
222 of CT hydrogenolysis by Fe(0) experiments at both pH values ($p < 0.0001$) (Fig. 2A). CT thiolytic
223 reduction evidenced by CS₂ formation is thus supported by means of C-Cl Λ . Moreover, since the
224 obtained Λ values in CT_Mag_12 and in CT experiments with Py were similar, a comparable
225 contribution of initial parallel reaction mechanisms for both reactions is hypothesized (hydrolytic and
226 thiolytic reduction, respectively Scheme S1).

227 **4. Conclusions**

228 CT and CF degradation by Fe(0) occurs at pH 7 and 12, with similar C-Cl Λ values at both pH values for
229 each compound (8 ± 2 and 8 ± 1 for CF; 6.1 ± 0.5 and 5.8 ± 0.4 for CT, respectively), pointing in both cases to
230 a hydrogenolysis pathway. Accumulation of recalcitrant DCM in this pathway should be taken into
231 consideration in remediation strategies by PRBs.

232 Isotope fractionation proved that under our experimental conditions, FeCl₂(aq), Mag and Py are effective
233 reducing agents for CT at pH 12, whereas at pH 7 only Py was able to degrade CT. CF was detected as
234 by-product in all CT-degrading experiments, while CS₂ was only detected with Py. The occurrence of
235 parallel CT hydrogenolysis and hydrolytic or thiolytic reduction pathways was also evidenced by the
236 dual-plot approach, showing CT experiments with FeCl₂(aq) and Mag at pH 12 (2 ± 1) and with Py
237 (2.9 ± 0.5 and 3.7 ± 0.9 at pH 7 and 12) Λ values different than that for hydrogenolysis alone with Fe(0)
238 (6.1 ± 0.5 at pH 7). Further CF and CS₂ degradation at pH 12 was confirmed through isotopic tracking,
239 reaffirming that by-products are not always traceable to confirm parent compound degradation. Mag and
240 Py are thus effective minerals for abiotic CT remediation strategies, especially under alkaline conditions,
241 where the accumulation of harmful by-products is avoided by further degradation. On the contrary, under
242 aquifer conditions, recycling these minerals for cost-effective PRB-building requires ensuring subsequent
243 CF and CS₂ elimination. The studied CMs degradation reactions might be diffusion-controlled under
244 natural field conditions, as it was previously reported (Elsner et al., 2007; Thullner et al., 2013). Thus,
245 due to this isotope masking by rate-limitations in mass transfer, the highest reported ϵ value should be
246 used for a conservative assessment of CMs degradation extent (Elsner et al., 2010; Thullner et al., 2012).
247 However, if these minerals or Fe(0) were used as remediation techniques, where a high
248 contaminant/mineral ratio is normally used, the C-Cl bond cleavage might be the rate-limiting step.
249 Nevertheless, further research would be needed to confirm this hypothesis.

250 To sum up, all the data provided in this dual element C-Cl isotopic approach – especially first-time-
251 published abiotic CT Δ values – in combination with earlier data for CF abiotic (Heckel et al., 2017a;
252 Torrentó et al., 2017) and CT and CF biotic transformation reactions (Rodríguez-Fernández et al., 2018),
253 improve considerably the isotopic database of CMs reactions. This information could be further applied in
254 field studies for discerning the predominant pathway or the contribution of combined pathways in CMs
255 natural attenuation following Van Breukelen (2007) or assessing the effect of remediation treatments over
256 time.

257 **Appendix A. Supplementary data**

258 Supplementary data to this article can be found online at:

259 **Acknowledgements**

260 This research was supported by a Marie Curie Career Integration Grant in the framework of IMOTEC-
261 BOX project (PCIG9-GA-2011-293808), REMEDIATION (CGL2014-57215-C4-1-R) and PACE
262 (CGL2017-87216-C4-1-R) both projects from Spanish Ministry of Economy and AEI/FEDER, UE as
263 well as the Catalan Government 2017SGR 1733 project. We thank technical support from CCiT-UB and
264 the work of the undergraduate students D.García and F.Bagaria. D.Rodríguez-Fernández acknowledges
265 FPU2012/01615 and Beca Fundació Pedro i Pons 2014 and M.Rosell, Ramón y Cajal contract (RYC-
266 2012-11920). We thank the editor and the anonymous reviewers for comments that improved the quality
267 of the manuscript.

268 **5. References**

- 269 Adewuyi, Y.G., Carmichael, G.R., 1987. Kinetics of hydrolysis and oxidation of carbon
270 disulfide by hydrogen peroxide in alkaline medium and application to carbonyl sulfide.
271 *Environ. Sci. Technol.* 21, 170–177. doi:10.1021/es00156a602
- 272 Amonette, J.E., Workman, D.J., Kennedy, D.W., Fruchter, J.S., Gorby, Y.A., 2000.
273 Dechlorination of carbon tetrachloride by Fe (II) associated with goethite. *Environ. Sci.*
274 *Technol.* 34, 4606–4613. doi:10.1021/es9913582
- 275 Arnold, W.A., Ball, W.P., Roberts, A.L., 1999. Polychlorinated ethane reaction with zero-valent
276 zinc: pathways and rate control. *J. Contam. Hydrol.* 40, 183–200. doi:10.1016/S0169-
277 7722(99)00045-5
- 278 Bonnissel-Gissinger, P., Alnot, M., Ehrhardt, J.J., Behra, P., 1998. Surface oxidation of pyrite as
279 a function of pH. *Environ. Sci. Technol.* 32, 2839–2845. doi:10.1021/es980213c
- 280 Breider, F., Albers, C.N., Hunkeler, D., 2013. Assessing the role of trichloroacetyl-containing
281 compounds in the natural formation of chloroform using stable carbon isotopes analysis.
282 *Chemosphere* 90, 441–448. doi:10.1016/j.chemosphere.2012.07.058
- 283 Burris, D.R., Campbell, T.J., Manoranjan, V.S., 1995. Sorption of trichloroethylene and
284 tetrachloroethylene in a batch reactive metallic iron-water system. *Environ. Sci. Technol.*
285 29, 2850–2855. doi:10.1021/es00011a022
- 286 Burris, D.R., Allen-King, R.M., Manoranjan, V.S., Campbell, T.J., Loraine, G.A., Deng, B.,
287 1998. Chlorinated ethene reduction by cast iron: sorption and mass transfer. *J. Environ.*
288 *Eng.* 124, 1012–1019. doi:10.1061/(ASCE)0733-9372(1998)124:10(1012)

- 289 Cappelletti, M., Frascari, D., Zannoni, D., Fedi, S., 2012. Microbial degradation of chloroform.
290 Appl. Microbiol. Biotechnol. 96, 1395–1409. doi:10.1007/s00253-012-4494-1
- 291 Choe, S., Lee, S.H., Chang, Y.Y., Hwang, K.Y., Khim, J., 2001. Rapid reductive destruction of
292 hazardous organic compounds by nanoscale Fe⁰. Chemosphere 42, 367–372.
293 doi:10.1016/S0045-6535(00)00147-8
- 294 Cretnik, S., Thoreson, K.A., Bernstein, A., Ebert, K., Buchner, D., Laskov, C., Haderlein, S.,
295 Shouakar-stash, O., Kliegman, S., McNeill, K., Elsner, M., 2013. Reductive dechlorination
296 of TCE by chemical model systems in comparison to dehalogenating bacteria: Insights
297 from dual element isotope analysis (¹³C/¹²C, ³⁷Cl/³⁵Cl). Environ. Sci. Technol. 47, 6855–
298 6863. doi:10.1021/es400107n
- 299 Danielsen, K.M., Hayes, K.F., 2004. pH dependence of carbon tetrachloride reductive
300 dechlorination by magnetite. Environ. Sci. Technol. 38, 4745–4752.
301 doi:10.1021/es0496874
- 302 Danielsen, K.M., Gland, J.L., Hayes, K.F., 2005. Influence of amine buffers on carbon
303 tetrachloride reductive dechlorination by the iron oxide magnetite. Environ. Sci. Technol.
304 39, 756–763. doi:10.1021/es049635e
- 305 Davis, A., Fennimore, G.G., Peck, C., Walker, C.R., McIlwraith, J., Thomas, S., 2003.
306 Degradation of carbon tetrachloride in a reducing groundwater environment: Implications
307 for natural attenuation. Appl. Geochemistry 18, 503–525. doi:10.1016/S0883-
308 2927(02)00102-6
- 309 Devlin, J.F., Muller, D., 1999. Field and laboratory studies of carbon tetrachloride
310 transformation in a sandy aquifer under sulfate reducing conditions. Environ. Sci. Technol.
311 33, 1021–1027. doi:10.1021/es9806884
- 312 Elsner, M., Haderlein, S.B., Kellerhals, T., Luzi, S., Zwank, L., Angst, W., Schwarzenbach,
313 R.P., 2004. Mechanisms and products of surface-mediated reductive dehalogenation of
314 carbon tetrachloride by Fe(II) on goethite. Environ. Sci. Technol. 38, 2058–2066.
315 doi:10.1021/es034741m
- 316 Elsner, M., Zwank, L., Hunkeler, D., Schwarzenbach, R.P., 2005. A new concept linking
317 observable stable isotope fractionation to transformation pathways of organic pollutants.
318 Environ. Sci. Technol. 39, 6896–6916. doi:10.1021/es0504587
- 319 Elsner, M., Cwiertny, D.M., Roberts, A.L., Sherwood Lollar, B., 2007. 1,1,2,2-
320 Tetrachloroethane reactions with OH⁻, Cr(II), granular iron, and a copper - iron bimetal:
321 insights from product formation and associated carbon isotope fractionation. Environ. Sci.
322 Technol. 41, 4111–4117. doi:10.1021/es072046z
- 323 Elsner, M., 2010. Stable isotope fractionation to investigate natural transformation mechanisms
324 of organic contaminants: principles, prospects and limitations. J. Environ. Monit. 12,
325 2005–2031. doi:10.1039/c0em00277a
- 326 Farrell, J., Kason, M., Melitas, N., Li, T., 2000. Investigation of the long-term performance of
327 zero-valent iron for reductive dechlorination of trichloroethylene. Environ. Sci. Technol.
328 34, 514–521. doi:10.1021/es990716y
- 329 Feng, J., Lim, T.T., 2005. Pathways and kinetics of carbon tetrachloride and chloroform
330 reductions by nano-scale Fe and Fe/Ni particles: Comparison with commercial micro-scale
331 Fe and Zn. Chemosphere 59, 1267–1277. doi:10.1016/j.chemosphere.2004.11.038
- 332 Feng, J., Zhu, B.-W., Lim, T.T., 2008. Reduction of chlorinated methanes with nano-scale Fe
333 particles: Effects of amphiphiles on the dechlorination reaction and two-parameter
334 regression for kinetic prediction. Chemosphere 73, 1817–1823.
335 doi:10.1016/j.chemosphere.2008.08.014
- 336 Ferrey, M.L., Wilkin, R.T., Ford, R.G., Wilson, J.T., 2004. Nonbiological removal of cis-
337 dichloroethylene and 1,1-dichloroethylene in aquifer sediment containing magnetite.
338 Environ. Sci. Technol. 38, 1746–1752. doi:10.1021/es0305609
- 339 Hanoch, R.J., Shao, H., Butler, E.C., 2006. Transformation of carbon tetrachloride by bisulfide
340 treated goethite, hematite, magnetite, and kaolinite. Chemosphere 63, 323–334.
341 doi:10.1016/j.chemosphere.2005.07.016
- 342 He, Y.T., Wilson, J.T., Su, C., Wilkin, R.T., 2015. Review of abiotic degradation of chlorinated
343 solvents by reactive iron minerals in aquifers. Groundw. Monit. Remediat. 35, 57–75.

344 doi:10.1111/gwmmr.12111

345 Heckel, B., Cretnik, S., Kliegman, S., Shouakar-Stash, O., McNeill, K., Elsner, M., 2017a.

346 Reductive outer-sphere single electron transfer is an exception rather than the rule in

347 natural and engineered chlorinated ethene dehalogenation. *Environ. Sci. Technol.* 51,

348 9663–9673. doi:10.1021/acs.est.7b01447

349 Heckel, B., Rodríguez-Fernández, D., Torrentó, C., Meyer, A., Palau, J., Domènech, C., Rosell,

350 M., Soler, A., Hunkeler, D., Elsner, M., 2017b. Compound-specific chlorine isotope

351 analysis of tetrachloromethane and trichloromethane by gas chromatography-isotope ratio

352 mass spectrometry vs gas chromatography-quadrupole mass spectrometry: method

353 development and evaluation of precision and trueness. *Anal. Chem.* 89, 3411–3420.

354 doi:10.1021/acs.analchem.6b04129

355 Helland, B.R., Alvarez, P.J.J., Schnoor, J.L., 1995. Reductive dechlorination of carbon

356 tetrachloride with elemental iron. *J. Hazard. Mater.* 41, 205–216. doi:10.1016/0304-

357 3894(94)00111-S

358 Hosono, T., Nakano, T., Shimizu, Y., Onodera, S. ichi, Taniguchi, M., 2011. Hydrogeological

359 constraint on nitrate and arsenic contamination in Asian metropolitan groundwater.

360 *Hydrol. Process.* 25, 2742–2754. doi:10.1002/hyp.8015

361 Huang, K.C., Zhao, Z., Hoag, G.E., Dahmani, A., Block, P.A., 2005. Degradation of volatile

362 organic compounds with thermally activated persulfate oxidation. *Chemosphere* 61, 551–

363 560. doi:10.1016/j.chemosphere.2005.02.032

364 Huling, S.G., Pivetz, B.E., 2006. In-Situ Chemical Oxidation-Engineering issue. EPA/600/R-

365 06/072. U.S. Environmental Protection Agency Office of Research and Development,

366 National Risk Management Research Laboratory: Cincinnati, OH.

367 Hunkeler, D., Laier, T., Breider, F., Jacobsen, O.S., 2012. Demonstrating a natural origin of

368 chloroform in groundwater using stable carbon isotopes. *Environ. Sci. Technol.* 46, 6096–

369 6101. doi:10.1021/es204585d

370 IARC, 1999. IARC Monographs on the evaluation of carcinogenic risks to humans 71, 319–

371 335.

372 Jeffers, P.M., Ward, L.M., Woytowlitch, L.M., Wolfe, N.L., 1989. Homogeneous hydrolysis rate

373 constants for selected chlorinated methanes, ethanes, ethenes, and propanes. *Environ. Sci.*

374 *Technol.* 23, 965–969. doi:10.1021/es00066a006

375 Kim, Y.H., Carraway, E.R., 2000. Dechlorination of pentachlorophenol by zero valent iron and

376 modified zero valent irons. *Environ. Sci. Technol.* 34, 2014–2017. doi:10.1021/es991129f

377 Koenig, J., Lee, M., Manefield, M., 2015. Aliphatic organochlorine degradation in subsurface

378 environments. *Rev. Environ. Sci. Bio/Technology* 14, 49–71. doi:10.1007/s11157-014-

379 9345-3

380 Kriegman-King, M.R., Reinhard, M., 1992. Transformation of carbon tetrachloride in the

381 presence of sulfide, biotite, and vermiculite. *Environ. Sci. Technol.* 26, 2198–2206.

382 doi:10.1021/es00035a019

383 Kriegman-King, M.R., Reinhard, M., 1994. Transformation of carbon tetrachloride by pyrite in

384 aqueous solution. *Environ. Sci. Technol.* 28, 692–700. doi:10.1021/es00053a025

385 Lee, M., Wells, E., Wong, Y.K., Koenig, J., Adrian, L., Richnow, H.H., Manefield, M., 2015.

386 Relative contributions of Dehalobacter and zerovalent iron in the degradation of

387 chlorinated methanes. *Environ. Sci. Technol.* 49, 4481–4489. doi:10.1021/es5052364

388 Lien, H.L., Zhang, W.X., 1999. Transformation of chlorinated methanes by nanoscale iron

389 particles. *J. Environ. Eng.* 125, 1042–1047. doi:10.1061/(ASCE)0733-

390 9372(1999)125:11(1042)

391 Lien, H.-L., Jhuo, Y.-S., Chen, L.-H., 2007. Effect of heavy metals on dechlorination of carbon

392 tetrachloride by iron nanoparticles. *Environ. Eng. Sci.* 24, 21–30.

393 doi:10.1089/ees.2007.24.21

394 Maithreepala, R.A., Doong, R., 2007. Dechlorination of carbon tetrachloride by ferrous ion

395 associated with iron oxide nano particles, in: *Proceedings of the Fourth Academic Sessions*

396 2007.

397 Martín-González, L., Mortan, S.H., Rosell, M., Parladé, E., Martínez-Alonso, M., Gaju, N.,

398 Caminal, G., Adrian, L., Marco-Urrea, E., 2015. Stable carbon isotope fractionation during

399 1,2-dichloropropane-to-propene transformation by an enrichment culture containing
400 *Dehalogenimonas* strains and a *dcpA* gene. *Environ. Sci. Technol.* 49, 8666–8674.
401 doi:10.1021/acs.est.5b00929

402 Matheson, L.J., Tratnyek, P.G., 1994. Reductive dehalogenation of chlorinated methanes by
403 iron metal. *Environ. Sci. Technol.* 28, 2045–2053. doi:10.1021/es00061a012

404 McGeough, K.L., Kalin, R.M., Myles, P., 2007. Carbon disulfide removal by zero valent iron.
405 *Environ. Sci. Technol.* 41, 4607–4612. doi:http://dx.doi.org/10.1021/es062936z

406 Morris, B.L., Lawrence, A.R.L., Chilton, P.J.C., Adams, B., C, C.R., Klinck, B.A., 2003.
407 Groundwater and its susceptibility to degradation: a global assessment of the problem and
408 options for management. Early Warning and Assessment Report Series, RS. 03-3., United
409 Nations Environment Programme. Nairobi, Kenya. doi:10.1017/CBO9781107415324.004

410 Nijenhuis, I., Renpenning, J., Kümmel, S., Richnow, H.H., Gehre, M., 2016. Recent advances in
411 multi-element compound-specific stable isotope analysis of organohalides: Achievements,
412 challenges and prospects for assessing environmental sources and transformation. *Trends*
413 *Environ. Anal. Chem.* 11, 1–8. doi:10.1016/j.teac.2016.04.001

414 Obiri-Nyarko, F., Grajales-Mesa, S.J., Malina, G., 2014. An overview of permeable reactive
415 barriers for in situ sustainable groundwater remediation. *Chemosphere* 111, 243–259.
416 doi:10.1016/j.chemosphere.2014.03.112

417 Palau, J., Marchesi, M., Chambon, J.C.C., Aravena, R., Canals, À., Binning, P.J., Bjerg, P.L.,
418 Otero, N., Soler, A., 2014. Multi-isotope (carbon and chlorine) analysis for
419 fingerprinting and site characterization at a fractured bedrock aquifer contaminated by
420 chlorinated ethenes. *Sci. Total Environ.* 475, 61–70.
421 doi:10.1016/j.scitotenv.2013.12.059

422 Pecher, K., Haderlein, S.B., Schwarzenbach, R.P., 2002. Reduction of polyhalogenated
423 methanes by surface-bound Fe(II) in aqueous suspensions of iron oxides. *Environ. Sci.*
424 *Technol.* 36, 1734–1741. doi:10.1021/es011191o

425 Penny, C., Vuilleumier, S., Bringel, F., 2010. Microbial degradation of tetrachloromethane:
426 mechanisms and perspectives for bioremediation. *FEMS Microbiol. Ecol.* 74, 257–275.
427 doi:10.1111/j.1574-6941.2010.00935.x

428 Peyton, T.O., Steel, R. V., Mabey, W.R., 1976. Carbon disulfide, carbonyl sulfide: literature
429 review and environmental assessment (EPA-600/9-78-009). Washington, DC.

430 Renpenning, J., Nijenhuis, I., 2016. Evaluation of the microbial reductive dehalogenation
431 reaction using Compound-Specific Stable Isotope Analysis (CSIA), in: Adrian, L., Löffler,
432 E.F. (Eds.), *Organohalide-Respiring Bacteria*. Springer Berlin Heidelberg, Berlin, pp. 429–
433 453. doi:10.1007/978-3-662-49875-0_18

434 Rodríguez-Fernández, D., Torrentó, C., Guivernau, M., Viñas, M., Hunkeler, D., Soler, A.,
435 Domènech, C., Rosell, M., 2018. Vitamin B₁₂ effects on chlorinated methanes-degrading
436 microcosms: dual isotope and metabolically active microbial populations assessment. *Sci.*
437 *Total Environ.* 621, 1615–1625. doi:10.1016/j.scitotenv.2017.10.067

438 Scherer, M.M., Balko, B.A., Tratnyek, P.G., 1998. The role of oxides in reduction reactions at
439 the metal-water interface, in: T, G. (Ed.), *Kinetics and Mechanisms of Reactions at the*
440 *Mineral/water Interface*, ACS Symposium Series, Division of Geochemistry. Washington,
441 DC, pp. 301–322.

442 Scheutz, C., Durant, N.D., Hansen, M.H., Bjerg, P.L., 2011. Natural and enhanced anaerobic
443 degradation of 1,1,1-trichloroethane and its degradation products in the subsurface - A
444 critical review. *Water Res.* 45, 2701–2723. doi:10.1016/j.watres.2011.02.027

445 Song, H., Carraway, E.R., 2006. Reduction of chlorinated methanes by nano-sized zero-valent
446 iron. Kinetics, pathways and effect of reaction conditions. *Environ. Eng. Sci.* 23, 272–284.
447 doi:10.1089/ees.2006.23.272

448 Svoronos, P.D.N., Bruno, T.J., 2002. Carbonyl Sulfide: A review of its chemistry and
449 properties. *Ind. Eng. Chem. Res.* 41, 5321–5336. doi:10.1021/ie020365n

450 Támara, M.L., Butler, E.C., 2004. Effects of iron purity and groundwater characteristics on rates
451 and products in the degradation of carbon tetrachloride by iron metal. *Environ. Sci.*
452 *Technol.* 38, 1866–1876. doi:10.1021/es0305508

453 Thullner, M., Centler, F., Richnow, H.H., Fischer, A., 2012. Quantification of organic pollutant

454 degradation in contaminated aquifers using compound specific stable isotope analysis -
455 Review of recent developments. *Org. Geochem.* 42, 1440–1460.
456 doi:10.1016/j.orggeochem.2011.10.011

457 Thullner, M., Fischer, A., Richnow, H.-H., Wick, L.Y., 2013. Influence of mass transfer on
458 stable isotope fractionation. *Appl. Microbiol. Biotechnol.* 97, 441–452.
459 doi:10.1007/s00253-012-4537-7

460 Torrentó, C., Audí-Miró, C., Bordeleau, G., Marchesi, M., Rosell, M., Otero, N., Soler, A.,
461 2014. The use of alkaline hydrolysis as a novel strategy for chloroform remediation: The
462 feasibility of using construction wastes and evaluation of carbon isotopic fractionation.
463 *Environ. Sci. Technol.* 48, 1869–1877. doi:10.1021/es403838t

464 Torrentó, C., Palau, J., Rodríguez-Fernández, D., Heckel, B., Meyer, A., Domènech, C., Rosell,
465 M., Soler, A., Elsner, M., Hunkeler, D., 2017. Carbon and chlorine isotope fractionation
466 patterns associated with different engineered chloroform transformation reactions.
467 *Environ. Sci. Technol.* 51, 6174–6184. doi:10.1021/acs.est.7b00679

468 Van Breukelen, B.M., 2007. Extending the Rayleigh equation to allow competing isotope
469 fractionating pathways to improve quantification of biodegradation. *Environ. Sci. Technol.*
470 41, 4004–4010. doi:10.1021/es0628452

471 Vikesland, P.J., Heathcock, A.M., Rebodos, R.L., Makus, K.E., 2007. Particle size and
472 aggregation effects on magnetite reactivity toward carbon tetrachloride. *Environ. Sci.*
473 *Technol.* 41, 5277–5283. doi:10.1021/es062082i

474 Vodyanitskii, Y.N., 2014. Effect of reduced iron on the degradation of chlorinated hydrocarbons
475 in contaminated soil and ground water: A review of publications. *Eurasian Soil Sci.* 47,
476 119–133. doi:10.1134/S1064229314020136

477 Zogorski, J.S., Carter, J.M., Ivahnenko, T., Lapham, W.W., Moran, M.J., Rowe, B.L., Squillace,
478 P.J., Toccalino, P.L., 2006. The quality of our nation's waters - Volatile organic
479 compounds in the nation's groundwater and drinking-water supply wells, U.S. Geological
480 Survey Circular 1292.

481 Zwank, L., Elsner, M., Aeberhard, A., Schwarzenbach, R.P., 2005. Carbon isotope fractionation
482 in the reductive dehalogenation of carbon tetrachloride at iron (hydr)oxide and iron sulfide
483 minerals. *Environ. Sci. Technol.* 39, 5634–5641. doi:10.1021/es0487776